Novel Design and Analysis of Aggregated ARQ Protocols for IEEE 802.11n Networks

Jia-Shi Lin, *Student Member*, *IEEE*, Kai-Ten Feng, *Member*, *IEEE*, Yu-Zhi Huang, and Li-Chun Wang, *Fellow*, *IEEE*

Abstract—The design of wireless local area networks (WLANs) with enhanced throughput performance have attracted significant amounts of attention in recent years. Based on the IEEE 802.11n standard, frame aggregation is considered one of the major factors to improve the system performance of WLANs from the medium access control (MAC) perspective. In order to fulfill the requirements of high throughput performance, feasible design of automatic repeat request (ARQ) mechanisms becomes important for providing reliable data transmission. In this paper, two MAC-defined ARQ protocols are proposed to consider the effect from frame aggregation for the enhancement of network throughput. An aggregated selective repeat ARQ (ASR-ARQ) scheme is proposed which incorporates the selective repeat ARQ scheme with the consideration of frame aggregation. On the other hand, for worse channel quality, the aggregated hybrid ARQ (AH-ARQ) mechanism is proposed to further enhance the throughput performance by adopting the Reed-Solomon (RS) block code as forward error correction (FEC) scheme. Novel analytical models for both the ASR-ARQ and AH-ARQ protocols are established with the consideration of interfering wireless stations. Simulations are conducted to validate and compare the proposed ARQ mechanisms based on the service time distribution and system throughput. Numerical evaluations show that the proposed AH-ARQ protocol can outperform the other schemes under worse channel condition; while the ASR-ARQ scheme is superior to the other mechanisms under better channel condition.

Index Terms—Wireless local area networks (WLAN), IEEE 802.11n standard, medium access control (MAC), automatic repeat request (ARQ), performance analysis

1 Introduction

In recent years, the techniques for wireless local area networks (WLANs) have been prevailing exploited for both indoor and mobile communications. The applications for WLANs include wireless home gateways, hotspots for commercial usages, and ad hoc networking for intervehicular communications. Among different techniques, the IEEE 802.11 standard is considered the well-adopted suite due to its remarkable success in both design and deployment. Various amendments are contained in the IEEE 802.11 standard suite, mainly including IEEE 802.11a/b/g [1], [2], [3] and IEEE 802.11e [4] for quality-of-service (QoS) support.

With increasing demands to support multimedia applications, the new amendment IEEE 802.11n [5], [6] has been proposed for achieving high throughput performance. The IEEE 802.11 task group N (TGn) enhances the PHY layer data rate up to 600 Mbps by adopting advanced communication techniques, such as multi-input multioutput (MIMO) technology [7]. It is noted that the MIMO technique utilizes spatial diversity to improve both the range and spatial multiplexing for achieving higher data rate. However, it has been investigated in [8] that simply improves the PHY data rate will not be sufficient for enhancing the system throughput from the medium access control (MAC) perspective. Accordingly, the IEEE 802.11 TGn further exploits frame aggregation and block acknowledgement (BA) techniques [6], [9] to moderate the drawbacks that are originated from the MAC/PHY overheads.

The benefits of adopting frame aggregation techniques have been studied from different perspectives [9], [10], [11], [12]. Without the consideration of retransmission mechanisms, simplified performance analysis considering frame aggregation has been conducted in [10] based on channel utilization. The dynamic frame aggregation scheme [11] adaptively changes the number of aggregated frames based on the channel conditions. Moreover, the multiuser polling controlled channel access (MCCA) protocol [12] performs both frame aggregation and multiuser polling in order to further enhance network utilization. Although the frame aggregation techniques can reduce both the transmission time of frame headers and the contention time induced by the random backoff period, the enlarged aggregated frames will cause other wireless stations (WSs) to wait for an elongated time period before their next opportunity for channel access. Furthermore, under the error-prone channels, corrupting an aggregated frame can result in the wastage of a longer channel access period which consequently leads to inferior throughput performance. Therefore, a feasible design of retransmission mechanisms becomes an important topic with the adoption of frame aggregation scheme.

The automatic repeat request (ARQ) [13], [14], [15] mechanisms have been extensively proposed in different wireless systems for reliable transmission. In order to reach

- *J.-S. Lin, K.-T. Feng, and L.-C. Wang are with the Department of Electrical and Computer Engineering, National Chiao Tung University, Hsinchu 300, Taiwan, R.O.C. E-mail: uxoxox.cm96g@g2.nctu.edu.tw, ktfeng@mail.nctu.edu.tw, lichun@cc.nctu.edu.tw.*
- *Y.-Z. Huang is with Holtek Semiconductor Incorporation, Hsinchu 300, Taiwan, R.O.C. E-mail: knight.cm95g@nctu.edu.tw.*

Manuscript received 12 Dec. 2009; revised 31 Jan. 2011; accepted 13 Jan. 2012; published online 31 Jan. 2012.
For information on obtaining reprints of this article, please send e-mail to: tmc@computer.org, and reference IEEECS Log Number TMC-2009-12-0537.
Digital Object Identifier no. 10.1109/TMC.2012.34.

more reliable transmissions within a shorter transmitting period, the hybrid ARQ (H-ARQ) schemes [16], [17], [18], [19], [20], which combine both the forward error correction (FEC) and retransmission mechanism, have been proposed for advanced multimedia applications. In general, the H-ARQ algorithms can be classified into three categories as follows: in the type-I H-ARQ scheme [18], as an error packet is detected via the cyclic redundancy check, the transmitter will retransmit the same packet either until the packet is successfully decoded at the receiver or a maximum retransmission limit is reached. Type-II of H-ARQ scheme is regarded as the full incremental redundancy (IR) technique [19], which decreases the coding rate in each retransmission by sending additional redundancy check digits. On the other hand, type-III of H-ARQ scheme [20], considered as a partial IR scheme, not only decrements the coding rate but also maintains the self-decoding capability in each retransmission. It is noted that the IR-based algorithms in general make use of either the rate compatible punctured convolutional (RCPC) codes [20], [21] or the rate compatible punctured turbo (RCPT) codes [22]. Furthermore, the transmission errors are corrected in two phases based on the design concept of concatenate code [23]. The inner decoder, which is implemented in the PHY layer, adopts sophisticated algorithms for error correction; while the outer decoder is served as the second stage fine-tuning error corrector that is implemented in the MAC layer protocols. As a consequence, the FEC schemes in both type-II and III of H-ARQ algorithms are regarded as the inner decoders; while that of type-I scheme is considered as the outer decoders.

However, most of the existing ARQ algorithms did not explicitly consider the effects from frame aggregation. Even though ARQ scheme is utilized for multiframe retransmission such as in [11], its design concept is primarily based on a pure stop-and-wait ARQ (SW-ARQ) mechanism. It is required to provide an efficient retransmission scheme in order to enhance the system throughput for the IEEE 802.11n networks. In this paper, MAC-defined ARQ mechanisms are proposed to consider the effect from frame aggregation in order to improve the network throughput. An aggregated selective repeat ARQ (ASR-ARQ) algorithm is proposed which incorporates the conventional selective repeat ARQ scheme with the consideration of frame aggregation. On the other hand, an aggregated hybrid ARQ (AH-ARQ) mechanism is proposed to further enhance the throughput performance for the IEEE 802.11n networks under worse channel quality. The proposed AH-ARQ scheme can be categorized as type-I of H-ARQ algorithm, which is served as an outer code designed from the MAC layer perspective. The Reed-Solomon (RS) code [24], [25], which defines a finite codeword length, is adopted within the AH-ARQ scheme.

Furthermore, it will be beneficial to construct effective analytical models to evaluate the retransmission mechanisms for the IEEE 802.11n networks. There are existing studies that propose analytical models for performance evaluation of the MAC channel access [26], [27], [28], [29] and frame aggregation techniques [30], [31], [32] in the IEEE 802.11-based networks. However, none of these models explicitly considers efficient retransmission schemes that are especially feasible for high throughput requirements. The studies in [33] and [34] investigate the impact of adopting block acknowledgement for high-speed WLANs and propose the analytical model for acquiring the system throughput. Nevertheless, these works did not construct the analytical models for aggregated packet delay distribution. Moreover, RS-based FEC mechanisms are adopted in [35], [36], and [37] for the purpose of reducing the frame error probability. Three error-control schemes are considered in [35] to compare the performance and computation complexity; while the scheme in [36] combines the retransmission scheme with a newly defined PHY format for enhancing the network performance. However, these analytical models only consider a single WS in the network that exclude the effect of channel contention between multiple WSs. Moreover, most of the existing studies did not include multiple opportunities for data transmission in one transmission opportunity (TXOP) that is allowed by the IEEE 802.11n standard.

As a consequence, with the consideration of multiple WSs, the service time distribution model with multiple transmission opportunities in one TXOP are constructed in order to observe the behaviors of both the ASR-ARQ and AH-ARQ algorithms. A novel approach based on the state diagram is utilized for the construction of analytical models for both schemes with the consideration of interfering WSs. Simulations are performed to both validate and compare the proposed ARQ schemes with conventional mechanism. It will be shown in the numerical results that the proposed AH-ARQ protocol can outperform the other mechanisms under worse channel condition; while the proposed ASR-ARQ scheme is superior to the other protocols under better channel condition.

The remainder of this paper is organized as follows: Section 2 describes the frame aggregation mechanism of IEEE 802.11n standard and the proposed ARQ algorithms. The system modeling and performance analysis of proposed ARQ schemes are addressed in Section 3. Section 4 provides the performance evaluation; while the conclusions are drawn in Section 5.

2 Proposed MAC-Defined Aggregated ARQ Schemes

In this section, the frame aggregation structure defined in the IEEE 802.11n MAC protocol is reviewed in Section 2.1. The proposed ASR-ARQ and AH-ARQ protocols are explained in Sections B and C, respectively.

2.1 Frame Aggregation/Deaggregation of IEEE 802.11n MAC Protocol

The IEEE 802.11n standard mandates the implementation of frame aggregation scheme for the sake of promoting transmission efficiency. It is noted that the transmission efficiency is defined as the time for delivering the information payload over the time duration for transmitting the entire aggregated frame associated with the required control frames and contention periods. With the frame format as shown in Fig. 1a, multiple MAC protocol data units (MPDUs) are combined into an aggregated

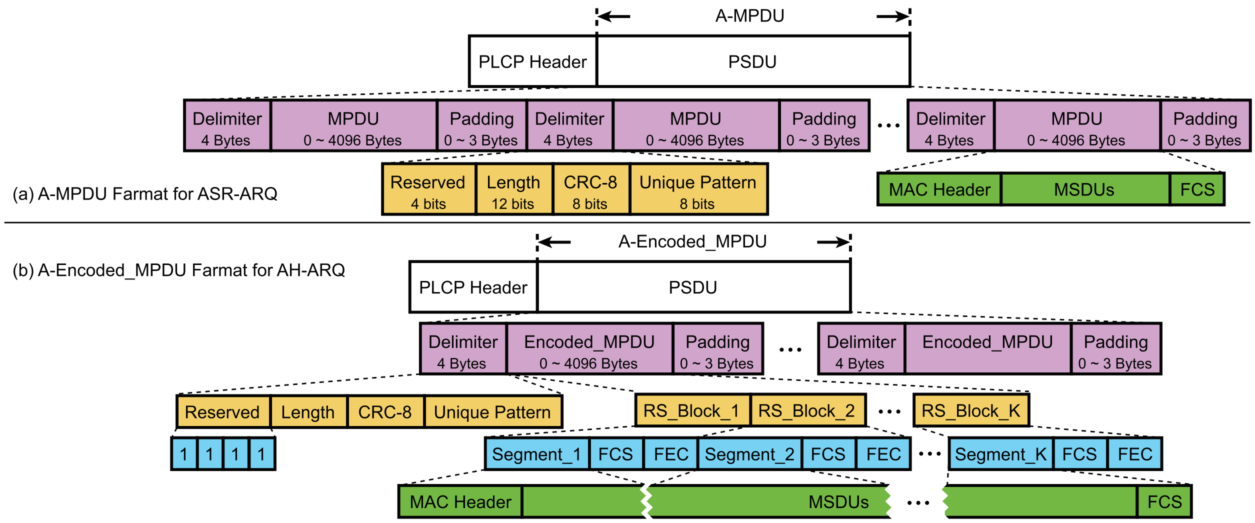

Fig. 1. (a) A-MPDU farmat for proposed ASR-ARQ scheme. (b) A-Encoded_MPDU farmat for proposed AH-ARQ scheme.

MPDU (A-MPDU), which is consequently transported into a single PHY service data unit (PSDU). Intuitively, the transmission efficiency can be improved with the utilization of A-MPDU since more MPDUs are transmitted with a communion of control overhead.

Each MPDU is padded with an MPDU delimiter for the purpose of extracting the corresponding MPDU from the aggregated frame. The extracting delimiter is composed of four bytes as shown in Fig. 1a, including the reserved, MPDU length, cyclic redundancy check (CRC), and unique pattern (UP) fields. It is noted that the UP field, which is set to the ASCII value of character "N," is employed to detect the location of an MPDU delimiter while scanning within the aggregated frame. Moreover, each MPDU is padded to become a multiple of four octets as shown in Fig. 1a. The deaggregation procedure at the receiver side described in the standard is shown in Fig. 2. The receiver verifies the validity of MPDU delimiter based on the 8-bits CRC and the observation of UP field, i.e., to exam the correctness of character "N." An MPDU can be successfully extracted from the A-MPDU if the corresponding MPDU delimiter is found to be valid. Otherwise, the de-aggregation process will continue to move forward with four bytes, i.e., via the offset parameter in Fig. 2, and to verify if the next multiple of four octets contains a valid delimiter.

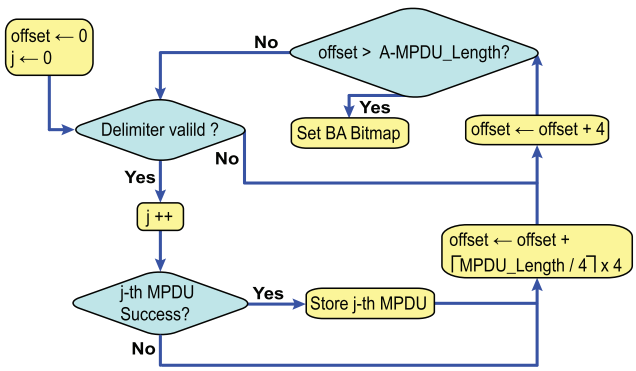

Fig. 2. The flow diagram of MPDUs deaggregation procedure for proposed ASR-ARQ scheme.

2.2 Proposed Aggregated Selective Repeat (ASR) ARQ Scheme

The design of retransmission mechanisms is an open topic from the standpoint of IEEE 802.11n standard. In this paper, the proposed ASR-ARQ scheme is enhanced from conventional selective repeat ARQ mechanism to consider frame aggregation within the design of retransmission algorithm. Contributing from the availability of BA scheme within the IEEE 802.11n standard, the ASR-ARQ algorithm can be effectively designed to provide transmission efficiency. Instead of sending individual acknowledgement (ACK) frame, the receiver replies with a BA frame for acknowledging the entire A-MPDU that is initiated from the transmitter. Since compressed BA is employed for this paper, the BA frame will consist of 32 octets that contain an 8-octets bitmap field. Each bit within the bitmap field identifies whether the corresponding MPDU from the aggregated frame has been correctly received. As shown in Fig. 2, the receiver will set the bitmap of BA after completing all the MPDU deaggregations and validations from an A-MPDU. Intuitively, a single BA frame can reduce the control overheads that are required by conventional design, which replies multiple ACK frames in response to an aggregated data frame.

In the proposed ASR-ARQ scheme, each MPDU within an A-MPDU is identified via a unique sequence number as the aggregated frame is transmitted. In the case that some of the MPDUs within an A-MPDU are missing during the transmission, the ASR-ARQ algorithm will continue to retransmit those unsuccessfully transmitted MPDUs until all the MPDUs have either been positively acknowledged by the BA frame or reached the retry limitation. For instance, there are 10 MPDUs contained within an A-MPDU that are identified by the sequence numbers from 1 to 10. If the MPDUs with sequence numbers 3 and 5 are corrupted and are identified via the CRC check, the receiver will reply with the BA frame which denotes two zero flags at the corresponding third and fifth bits within the bitmap field. A new A-MPDU, which includes only the third and fifth MPDUs, will be delivered by the transmitter at the next transmission opportunity. The retransmission procedure terminates until either all the MPDUs with sequence numbers from 1 to 10 are correctly accepted by the receiver or the maximum number of retransmission trials (i.e., identified by the Retry_Limit parameter) has achieved.

2.3 Proposed Aggregated Hybrid (AH) ARQ Scheme

In order to further enhance the transmission efficiency, the AH-ARQ scheme is proposed in this paper to integrate both the RS-based FEC construction and deaggregated retransmission mechanism, which are described in the next two sections.

2.3.1 RS-Based FEC Construction

With the compliance to existing IEEE 802.11n MAC frame structure, the proposed FEC mechanism is constructed according to the RS code [24], [25] that is well-adopted in the design of outer decoders. The coefficients of generator polynomial $G(x)$ are elements in a finite field $GF(2^{n_b})$, where $n_b = 8$ is chosen according to the byte-oriented system. For a RS (n_c, n_i) code with $n_c = 2^{n_b} - 1 = 255$ as the codeword length, n_i as the size of original information symbols, and $\theta = (n_c - n_i)/2$ as the error correction capability, the set of roots $\boldsymbol{\alpha} = \{\alpha, \alpha^2, \ldots, \alpha^{2\theta}\}$ of $G(x)$ is selected from $GF(2^8)$ where α is a primitive element of the finite field. As a result, the generator polynomial $G(x)$ can be represented as $G(x) = \prod_{i=1}^{2\theta}(x + \alpha^i) = x^{2\theta} + \sum_{i=0}^{2\theta-1} g_i x^i$ with g_i representing the coefficients for all $i \in \{0, \ldots, 2\theta - 1\}$. Based on the cyclic property of RS code, the set of codewords can be formed with the multiplication of both $G(x)$ and the information symbol polynomial $I(x)$. Moreover, the RS code will have the minimum codeword distance $d_{min} \geq 2\theta + 1$ in the case that all the coefficients g_i are not equal to zero. Therefore, the corresponding RS code possesses the correcting capability of θ error symbols associated with the codeword length of n_c octets and n_i information octets. There are total of $n_c - n_i = 2\theta$ parity check octets, which are served as the remainder $R(x)$ while dividing $x^{2\theta} I(x)$ by the generator polynomial $G(x)$.

2.3.2 Deaggregation and Retransmission Mechanism

A newly defined Aggregated-Encoded_MPDU (A-Encoded_MPDU) structure for the proposed AH-ARQ scheme is illustrated in Fig. 1b. The original MPDU, including MAC header, MSDUs, and FCS, is divided as several segments each with $(n_i - 4)$ bytes, and the CRC-32 value can be calculated as the FCS and is attached after each segment to verify its correction. Moreover, the FEC value is computed according to both the segment and FCS in order to implement forward error correction. Note that the total size for a RS block, including segment, FCS, and FEC, will be $(n_i - 4) + 4 + 2\theta = 255$ bytes. Furthermore, a series of zeros will be padded after the original MPDU such that its size will become the multiple of $(n_i - 4)$ bytes. The receiver can acquire the original size of the MPDU according to the Length field of the delimiter. In order to extract the A-Encoded_MPDUs that adopt the FEC mechanism, a modified deaggregation procedure is performed as shown in Fig. 3. At the beginning, the scanning process will start to search for the UP field. After the UP has been identified, a predefined symbol will be traversed in order to verify the

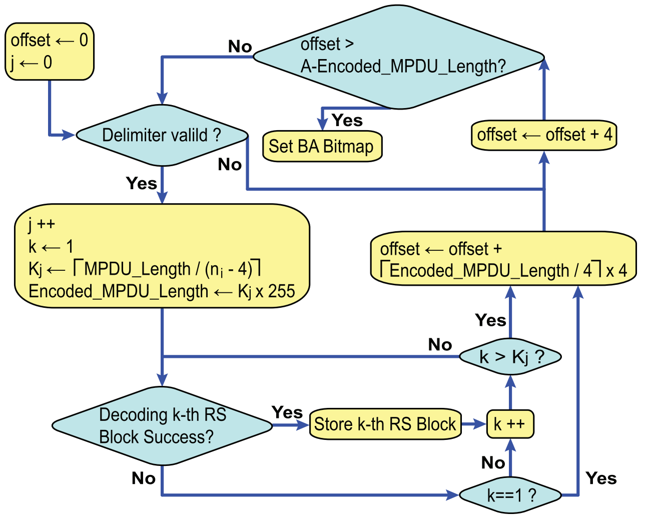

Fig. 3. The flow diagram of Encoded_MPDUs deaggregation procedure for proposed AH-ARQ scheme.

usage of FEC scheme. In other words, a valid delimiter will be identified if both the reserved field within the delimiter matches the "1111," i.e., "0xF," and the CRC-8 value is determined correct. The receiver can start to execute the deaggregation procedure if all the verifications are valid. The number of RS blocks for the jth Encoded_MPDU can be calculated as

$$K_j = \left\lceil \frac{MPDU\_Length_j}{n_i - 4} \right\rceil, \tag{1}$$

where the $MPDU\_Length_j$ is obtained from the Length field of jth delimiter. Therefore, the receiver will be aware of the size of jth Encoded_MPDU, i.e., equal to $K_j \times 255$, and also the location of the next delimiter. The next step is to execute the CRC-32 validation for each RS block in the Encoded_MPDU. If the result is valid, the receiver can store the RS block directly. Otherwise, the RS decoding procedure will be performed for this RS block. Note that the Berlekamp's iterative algorithm [38] is adopted to implement the decoding procedure. After completing the decoding process, the receiver will execute the CRC-32 check to verify if the decoded RS block can pass the verification. If not, this RS block will be dropped.

After all the Encoded_MPDUs have been extracted with all RS blocks been processed, the receiver starts to set the bits within the BA frame's bitmap field that map to the corresponding RS blocks. Considering a common scenario that the number of RS blocks in each Encoded_MPDU is a fixed value, i.e., $K_j = K$, the bitmap field within the BA for the proposed AH-ARQ protocol is extended to contain 256 bits in order to support J Encoded_MPDUs with K, $K \leq 256/J$, RS blocks in each Encoded_MPDU for a single data transmission. If the RS blocks are either correctly received or with correctable errors, the receiver will enable the corresponding bits in the bitmap field of BA frame. Otherwise, these bits will be disabled. The receiver will reply a BA frame to the transmitter after finishing setting up the bitmap of BA. The transmitter can initiate a retransmission of failed RS blocks according to the received BA. Note that all the RS blocks in the Encoded_MPDU can be considered independently, except for the first RS block. It is required for the entire Encoded_MPDU to be retransmitted if the first RS block fails in transmission since it contains the MAC header information of the Encoded_MPDU. The receiver cannot recognize the remaining RS blocks without the MAC header. Moreover, the first RS block is always needed in the Encoded_MPDU to provide important information, e.g., the receiver address, if there exists at least one other RS block in this Encoded_MPDU that should be retransmitted.

3 Performance Analysis of Proposed ARQ Schemes with Existence of Interfering Stations

In this section, novel analytical models based on the state diagram are exploited to analyze the performance of proposed ASR-ARQ and AH-ARQ mechanisms under saturated traffic. The service time distributions for both ARQ schemes are acquired with the consideration of interfering stations in the network. Distributed network topology is considered, where there are one access point (AP) and N WSs. The N WSs are contending for channel access in order to communicate with the AP for data transmission. Furthermore, the distributed coordination function (DCF) is employed as the medium access scheme for one access category between the transmitter and the receiver. The request-to-send/clear-to-send (RTS/CTS) mechanism is used for channel reservation in order to enhance the basic access mechanism. The proposed analytical models can be applied to all the N WSs contending the channel access. Moreover, the proposed models are also suitable for both the N WSs and the AP since all of them adopt the same contention-based protocol, e.g., the RTS/CTS handshaking and the backoff process. If the AP has data to be delivered to the WSs, the AP's behavior can be obtained by replacing the number N with $N+1$ in the analytical models since the number of total stations that contend the channel will include N WSs and one AP. Subsection A described the service model for contention-based systems. Subsection B explains the modeling of service time distribution for the proposed ASR-ARQ scheme; while that of the AH-ARQ algorithm is presented in Section 3.3.

3.1 Service Model for Contention-Based Systems

There are existing research [26], [39], [40], [41], [42], [43] establishing the analytical models for the backoff process of DCF scheme under different considerations, e.g., fading channel [39], backoff suspension [42], or retry limit [43]. The 2D Markov chain model is adopted as the baseline model to analyze the channel contention behaviors for the proposed ARQ mechanisms. As shown in Fig. 4, $W_i = 2^i W$ is defined as the backoff window size at the stage i where W denotes the minimum backoff window size. According to the DCF-based system, the steady state probability $b_{i,k}$ for the WS can be derived from the Markov chain model, where the subscript (i,k) indicates that the WS is at the ith backoff stage with its backoff counter equal to k. Therefore, the state probability $b_{i,k}$ can be inferred as

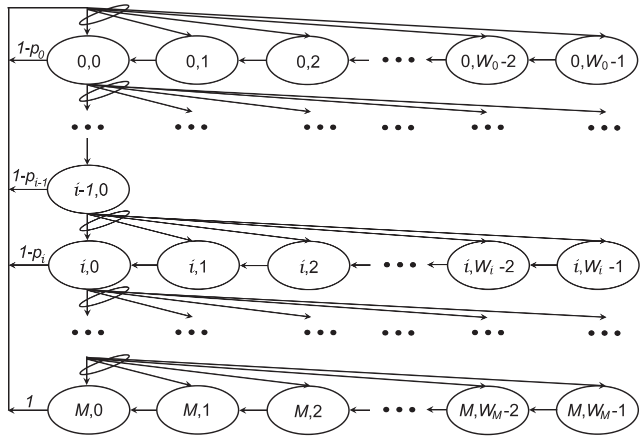

Fig. 4. Two-dimensional Markov chain model for the backoff process of contention-based systems.

$$\begin{cases} P(b_{i,k}|b_{i,k+1}) = 1, & 0 \le k \le W_i - 2, 0 \le i \le M, \\ P(b_{0,k}|b_{i,0}) = \dfrac{1-p_i}{W_0}, & 0 \le k \le W_0 - 1, 0 \le i \le M-1, \\ P(b_{0,k}|b_{M,0}) = \dfrac{1}{W_0}, & 0 \le k \le W_0 - 1, \\ P(b_{i,k}|b_{i-1,0}) = \dfrac{p_{i-1}}{W_i}, & 0 \le k \le W_i - 1, 1 \le i \le M, \end{cases} \tag{2}$$

where M denotes the maximum number of backoff stage. Note that the retry limit is assumed equal to M in this paper. Moreover, the parameter p_i represents the failed transmission probability at the ith stage. Each steady state probability can be expressed as a function of $b_{0,0}$ based on the equations in (2). Since the sum of all the states will be equal to 1, namely $\sum_{i=0}^{M}\sum_{k=0}^{W_i-1} b_{i,k} = 1$, $b_{0,0}$ can be obtained as

$$b_{0,0} = \left\{ \frac{W+1}{2}\left[1 - p_0 + \sum_{i=1}^{M-1}\left((1-p_i)\prod_{j=0}^{i-1} p_j\right) + \prod_{i=0}^{M-1} p_i\right] + \sum_{i=1}^{M}\left(\frac{2^i W + 1}{2}\prod_{j=0}^{i-1} p_j\right)\right\}^{-1}. \tag{3}$$

Let τ be defined as the probability that a WS transmits an RTS packet in a randomly selected time slot. Based on the model in Fig. 4, a WS can transmit its RTS packets only if the backoff counter k reaches zero. Therefore, the parameter τ can be acquired as

$$\tau = \sum_{i=0}^{M} b_{i,0} = \left[1 + \left(\sum_{i=1}^{M}\prod_{j=0}^{i-1} p_j\right)\right] b_{0,0}. \tag{4}$$

Let P_c represent the probability that the RTS packet issued by one WS collides with those from the other WSs, which can be calculated as

$$P_c = 1 - (1-\tau)^{N-1}. \tag{5}$$

Combining (3), (4), and (5), it is observed that P_c is a function of p_i for $0 \le i < M$. In order to solve these unknown parameters, it is required to provide another relationship between p_i and P_c. It is assumed that each WS possesses a saturated queue, and there exists J aggregated MPDUs in each transmission at the initial, i.e., the 0th, backoff stage. The WS will retransmit the failed MPDUs

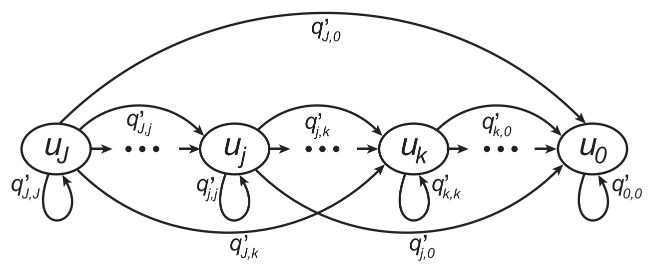

Fig. 5. State diagram for the proposed ASR-ARQ and AH-ARQ schemes.

within the A-MPDU until either all the MPDUs are successfully received or the backoff stage has achieved the retry limit. Therefore, the state diagram for transmitting the failed MPDUs in one TXOP period can be modeled as shown in Fig. 5, where u_j indicates the state of j unsuccessful MPDUs and $q'_{j,k}$ represents the transition probability from state u_j to u_k. In other words, suppose that there are j failed MPDUs at the beginning of the TXOP, the probability that there still exists k failed MPDUs at the end of the TXOP is equal to $q'_{j,k}$. Considering that there are L opportunities for transmitting an A-MPDU in the TXOP, the transition probabilities $q'_{j,k}$ can be formulated as

$$\begin{pmatrix} q'_{j,0} \\ q'_{j,1} \\ \vdots \\ q'_{j,j} \end{pmatrix} = (1-P_c)\cdot \begin{pmatrix} q_{j,0}(1) \\ q_{j,1}(1) \\ \vdots \\ q_{j,j}(1) \end{pmatrix} + P_c \cdot \begin{pmatrix} 0 \\ \vdots \\ 0 \\ 1 \end{pmatrix}, \tag{6}$$

where

$$\begin{pmatrix} q_{j,0}(z) \\ q_{j,1}(z) \\ \vdots \\ q_{j,j}(z) \end{pmatrix} = \mathbf{H}^L \cdot \begin{pmatrix} 0 \\ \vdots \\ 0 \\ 1 \end{pmatrix}, \tag{7}$$

where

$$\mathbf{H} = \begin{pmatrix} 1 & C_0^1(1-P_e)\cdot z^{T_{D,M}} & \dots & C_0^j(1-P_e)^j \cdot z^{j\cdot T_{D,M}} \\ 0 & C_1^1 P_e \cdot z^{T_{D,M}} & \dots & C_1^j P_e(1-P_e)^{j-1}\cdot z^{j\cdot T_{D,M}} \\ \vdots & \vdots & \ddots & \vdots \\ 0 & 0 & \dots & C_j^j P_e^j \cdot z^{j\cdot T_{D,M}} \end{pmatrix}.$$

Note that P_c is obtained from (5), and $T_{D,M}$ represents the required time for delivering both the delimiter and MPDU. The parameter P_e is equal to $P_{MPDU} + P_{DEL} - P_{MPDU}\cdot P_{DEL}$, where P_{MPDU} and P_{DEL} represent the probability of MPDU error and delimiter error, respectively. Note that $q_{j,k}(z)$ in (7) stands for the transition probability along with its required time in the power of z from state u_j to u_k without the consideration of RTS placket collisions. Moreover, it is noted that the WS is not able to transmit the MPDUs if its RTS packet collides with the other WSs in the network. At the ith backoff stage, let $\alpha_{i,j}$ be denoted as the probability that there still exists j failed MPDUs after either the WS successfully sends its RTS packet and the corresponding A-MPDU or the RTS packet is failed in transmission. Therefore, $\alpha_{i,j}$ can be calculated based on the following $(J+1)\times(J+1)$ matrix operation as

$$\begin{pmatrix} \alpha_{i,0} \\ \alpha_{i,1} \\ \vdots \\ \alpha_{i,J} \end{pmatrix} = \begin{pmatrix} q'_{0,0} & q'_{1,0} & \dots & q'_{J,0} \\ 0 & q'_{1,1} & \dots & q'_{J,1} \\ \vdots & \vdots & \ddots & \vdots \\ 0 & 0 & \dots & q'_{J,J} \end{pmatrix}^{i+1} \cdot \begin{pmatrix} 0 \\ \vdots \\ 0 \\ 1 \end{pmatrix}. \tag{8}$$

Finally, the probability of unsuccessful transmission at the ith backoff stage, i.e., p_i, can be formulated as

$$p_i = \begin{cases} 1-\alpha_{0,0}, & i = 0, \\ \dfrac{1-\alpha_{i,0}}{1-\alpha_{i-1,0}}, & 0 < i \le M. \end{cases} \tag{9}$$

Combining (6), (8), and (9), the parameter p_i can be regarded as functions of P_c. Therefore, by iteratively solving the nonlinear functions (4) and (5), the two parameters τ and P_c can be obtained. Moreover, the parameters $q'_{j,k}$, $\alpha_{i,j}$, and p_i can also be calculated.

3.2 Modeling of Service Time Distribution for Proposed ASR-ARQ Scheme

In this section, the derivation of service time distribution for the WS will be described based on the proposed ASR-ARQ scheme under the existence of contending stations. Let $S_i(z)$ be defined as the probability generating function (PGF) of service time distribution on the condition that all the MPDUs are successfully received at the ith backoff stage. Furthermore, let $F_{i,j}(z)$ represent the PGF of total required time distribution on the condition that there are j $(j \neq 0)$ failed MPDUs at the ith backoff stage. Note that both $S_i(z)$ and $F_{i,j}(z)$ do not include the backoff delay. Therefore, these two distributions can be formulated as

$$\begin{aligned} S_0(z) &= \frac{1-P_c}{\alpha_{0,0}}\cdot q_{J,0}(z)\cdot z^{T_A}, \\ S_i(z) &= \frac{1-P_c}{\alpha_{i,0}-\alpha_{i-1,0}} \left(\sum_{j=1}^{J} \alpha_{i-1,j}\cdot F_{i-1,j}(z)\cdot q_{j,0}(z) \right) \\ &\quad \cdot z^{T_A}, \quad 0 < i \le M, \end{aligned} \tag{10}$$

and

$$\begin{aligned} F_{0,J}(z) &= \frac{1}{\alpha_{0,J}}\left[(1-P_c)\cdot q_{J,J}(z)\cdot z^{T_A} + P_c \cdot z^{T_{out}}\right], \\ F_{0,j}(z) &= \frac{1-P_c}{\alpha_{0,j}}\cdot q_{J,j}\cdot z^{T_A},\ 0 < j < J, \\ F_{i,j}(z) &= \frac{1-P_c}{\alpha_{i,j}}\left[\sum_{r=j}^{J}\alpha_{i-1,r}\cdot F_{i-1,r}(z)\cdot q_{r,j}(z)\cdot z^{T_A}\right], \\ &\quad + \frac{P_c}{\alpha_{i,j}}\cdot \alpha_{i-1,j}\cdot F_{i-1,j}(z)\cdot z^{T_{out}},\ 0 < i \le M,\ 0 < j < J, \end{aligned} \tag{11}$$

where

$$\begin{aligned} T_A = {} & T_{DIFS} + T_{RTS} + T_{CTS} + L\cdot T_{PHY\_Header} \\ & + L\cdot T_{BA} + (2L+1)\cdot T_{SIFS} + (2L+2)\cdot\delta. \end{aligned}$$

The parameter $T_{out} = T_{DIFS} + T_{RTS} + T_{CTS} + T_{SIFS} + 2\delta$ denotes the required timeout interval. Note that the parameters T_{DIFS}, T_{SIFS}, T_{RTS}, T_{CTS}, T_{PHY_Header}, T_{BA}, and δ are defined as the required time intervals for DIFS, SIFS, RTS packet transmission, CTS packet transmission, PHY header

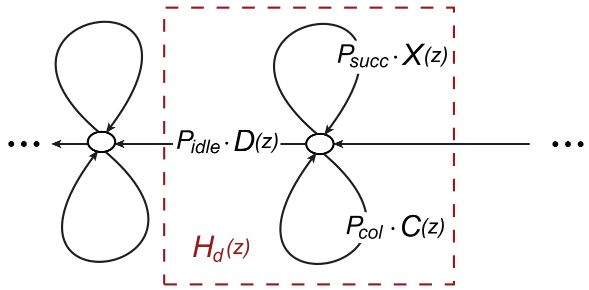

Fig. 6. Schematic diagram for the PGF of slot time delay distribution $H_d(z)$.

transmission, and propagation delay, respectively. Note also that (10) and (11) are approximated forms since a total of L opportunities are assumed for A-MPDU transmissions in a TXOP. In reality, the WS will not utilize the rest of transmission opportunities if all its MPDUs have been successfully transmitted. Furthermore, considering that there exists a specific WS in the backoff process, three exclusive events may occur in a slot time as follows: 1) there does not exist any other WS that sends the RTS packet; 2) there only exists one other WS sending its RTS packet; and 3) there exists at least two other WSs that send out their RTS packets. Let P_{idle}, P_{succ}, and P_{col} be denoted as the probability for events (a), (b), and (c) to occur in a slot time, which can, respectively, be calculated as

$$\begin{cases} P_{idle} = (1-\tau)^{N-1}, \\ P_{succ} = (N-1)\tau(1-\tau)^{N-2}, \\ P_{col} = 1-(1-\tau)^{N-1} - (N-1)\tau(1-\tau)^{N-2}. \end{cases} \quad (12)$$

On the condition that a specific WS is in the backoff process, P_{col} denotes the probability that at least two of the other $(N-1)$ WSs contend the channel unsuccessfully due to the RTS packet collisions. Note that P_{col} is different from P_c in (5) which indicates the collision probability on the condition that the RTS packet is delivered by this specific WS. It is noticed that the reason for calculating (12) is to formulate the PGF of slot time delay distribution $H_d(z)$ from the backoff delay as illustrated in Fig. 6, where $D(z)$, $X(z)$, and $C(z)$ are denoted as the PGF of required time distribution given the event (a), (b), and (c), respectively. Therefore, $H_d(z)$ can be derived as

$$\begin{aligned} H_d(z) &= P_{idle}D(z) + P_{succ}X(z)H_d(z) + P_{col}C(z)H_d(z) \\ \Rightarrow \; H_d(z) &= \frac{P_{idle} \cdot D(z)}{1 - P_{succ} \cdot X(z) - P_{col} \cdot C(z)}. \end{aligned} \quad (13)$$

It is also noted that Fig. 6 can be considered as an extension of the original Markov chain model in Fig. 4 to further account for the delay time distribution. In other words, Fig. 4 is utilized to analytically compute the system throughput which can be simplified from Fig. 6 by setting $P_{idle} = 1$ in a slot time, i.e., only event (a) will occur in a slot time such that the time delays costs from the PGFs $D(z)$, $X(z)$, and $C(z)$ are not considered. On the other hand, it is considered computationally complex to calculate (13) owing to the complexity in the denominator, i.e., $1 - P_{succ} \cdot X(z) - P_{col} \cdot C(z)$. In order to reduce the complicated computation, events (b) and (c) are assumed to occur at most once in a backoff time slot. Therefore, (13) can be approximated as

$$H_d(z) \approx P_{idle} \cdot D(z) + P_{succ} \cdot X(z)D(z) + P_{col} \cdot C(z)D(z). \quad (14)$$

Moreover, the expressions of $D(z)$, $X(z)$, and $C(z)$ can be obtained as

$$\begin{cases} D(z) = z^{\sigma}, \\ X(z) = \sum_{i=0}^{M} \frac{b_{i,0}}{\tau} \sum_{j=1}^{J} \left[P_{X,i,j} \cdot \left(\sum_{r=0}^{j} q_{j,r}(z) \cdot z^{T_A} \right) \right], \\ C(z) = z^{T_{out}}, \end{cases} \quad (15)$$

where

$$P_{X,i,j} = \begin{cases} 1, & i=0, \; j=J, \\ 0, & i=0, \; 0<j<J, \\ \frac{\alpha_{i-1,j}}{1-\alpha_{i-1,0}}, & 0<i\le M, \; 0<j\le J, \end{cases} \quad (16)$$

and the parameter σ represents a slot time. Consequently, the total backoff delay at the ith backoff stage, $H_i(z)$, can be derived as

$$H_i(z) = \frac{1}{2^i W} \sum_{r=0}^{2^i W - 1} \left(H_d(z)\right)^r, \; 0 \le i \le M. \quad (17)$$

Let $\phi_{succ,i}$ indicates the probability that all the MPDUs have been successfully received at the ith backoff stage, which can be calculated as

$$\phi_{succ,i} = \begin{cases} \alpha_{0,0}, & i=0, \\ \alpha_{i,0} - \alpha_{i-1,0}, & 0<i\le M, \end{cases} \quad (18)$$

As a result, the PGF of total service time distribution $T(z)$ can be obtained as

$$\begin{aligned} T(z) = &\left(\sum_{i=0}^{M} \phi_{succ,i} \cdot S_i(z) \cdot \prod_{r=0}^{i} H_r(z) \right) \\ &+ \left(\sum_{j=1}^{J} \alpha_{M,j} \cdot F_{M,j}(z) \right) \prod_{r=0}^{M} H_r(z), \end{aligned} \quad (19)$$

where the parameter $\alpha_{M,j}$, which can be obtained in (8), denotes the probability of j failed MPDUs that are dropped after reaching the retry limit.

3.3 Modeling of Service Time Distribution for Proposed AH-ARQ Scheme

In this section, the performance analysis and modeling for the service time distribution of proposed AH-ARQ scheme is presented. Based on the RS code, the decoding errors occur while there are more than θ corrupted symbols within a predefined block. Therefore, a decoding error probability B_e of a block can be formulated as

$$B_e = \sum_{r=\theta+1}^{n_c} C_r^{n_c} s_e^r (1-s_e)^{n_c - r}. \quad (20)$$

The parameter s_e represents the error rate of an RS symbol defined in $GF(2^{n_b})$ with n_b bits, i.e., $s_e = 1 - (1 - \text{BER})^{n_b}$ where BER denotes the bit error rate. It is noticed that B_e as defined in (20) is usually served as an upper bound of decoding errors for the RS code. Let H_e be denoted as the probability that either the delimiter or the first RS block in the Encoded_MPDU fails in transmission, which can be calculated as

$$H_e = B_e + P_{DEL} - B_e \cdot P_{DEL}. \tag{21}$$

Note again that the entire Encoded_MPDU should be retransmitted if either the delimiter or the first RS block fails in transmission. Within an A-Encoded_MPDU, it is assumed that there are J Encoded_MPDUs and each has K RS blocks. In order to distinguish the first RS block and the remaining RS blocks, the parameter $K' = K - 1$ is utilized to indicate the number of remaining RS blocks in an Encoded_MPDU, and K' will start from two for identifying each RS block. Refer to Fig. 5, let $\widetilde{u}_k$ be defined as the state of k failed RS blocks in a specific Encoded_MPDU, and $\widetilde{q'}_{k,l}$ represents the transition probability from the state $\widetilde{u}_k$ to $\widetilde{u}_l$ in a single A-Encoded_MPDU transmission. The probability $\widetilde{q'}_{k,l}$ can be formulated as

$$\widetilde{q'}_{k,l} = \begin{cases} H_e + (1 - H_e)B_e^k, & k = l, \\ (1 - H_e) \cdot B_e^l (1 - B_e)^{k-l}, & k > l, \\ 0, & k < l, \end{cases} \tag{22}$$

for $0 \le k, l \le K'$. Note that $\widetilde{q'}_{k,l}$ is defined for a single A-Encoded_MPDU transmission transmission given the successful transmission of the RTS packet. Hence, $\widetilde{q}_{k,l}(z)$, the transition probability along with required time in the power of z from state $\widetilde{u}_k$ to $\widetilde{u}_l$ in the L opportunities for A-Encoded_MPDU transmissions, can be derived as

$$\begin{pmatrix} \widetilde{q}_{k,0}(z) \\ \widetilde{q}_{k,1}(z) \\ \vdots \\ \widetilde{q}_{k,k}(z) \end{pmatrix} = \begin{pmatrix} 1 & \widetilde{q'}_{1,0} \cdot z^{T_{RS}} & \dots & \widetilde{q'}_{k,0} \cdot z^{k \cdot T_{RS}} \\ 0 & \widetilde{q'}_{1,1} \cdot z^{T_{RS}} & \dots & \widetilde{q'}_{k,1} \cdot z^{k \cdot T_{RS}} \\ \vdots & \vdots & \ddots & \vdots \\ 0 & 0 & \dots & \widetilde{q'}_{k,k} \cdot z^{k \cdot T_{RS}} \end{pmatrix}^L \cdot \begin{pmatrix} 0 \\ \vdots \\ 0 \\ 1 \end{pmatrix}, \tag{23}$$

where the parameters T_{RS} represents the transmission time of one RS block. Moreover, let x_j for $0 \le x_j \le K'$ be denoted as the number of failed RS blocks except for the first one in the jth Encoded_MPDU, which are integrated into the vector $\mathbf{x} = [x_1\ x_2\ \dots\ x_j\ \dots\ x_J]$ for $1 \le j \le J$. Furthermore, at the ith backoff stage, let $\widetilde{\alpha}_{i,\mathbf{x}}$ be denoted as the probability that there are still x_j failed RS blocks in the jth Encoded_MPDU for $1 \le j \le J$ after either the WS successfully sends its RTS packet and the corresponding A-MPDU or the RTS packet is failed in transmission, which can be derived as

$$\begin{aligned} &\widetilde{\alpha}_{0,\mathbf{x}} = P_c + (1 - P_c) \cdot (\widetilde{q}_{K',K'}(1))^J,\ i = 0,\ \mathbf{x} = K' \cdot \mathbf{1}, \\ &\widetilde{\alpha}_{0,\mathbf{x}} = (1 - P_c) \cdot \left[\prod_{j=1}^{J} \widetilde{q}_{K',x_j}(1) \right],\ i = 0,\ \mathbf{x} \ne K' \cdot \mathbf{1}, \\ &\widetilde{\alpha}_{i,\mathbf{x}} = P_c \cdot \widetilde{\alpha}_{i-1,\mathbf{x}} + (1 - P_c) \sum_{\mathbf{r} \in \mathbf{U_x}} \left[\widetilde{\alpha}_{i-1,\mathbf{r}} \cdot \prod_{j=1}^{J} \widetilde{q}_{r_j,x_j}(1) \right], \\ &\qquad 0 < i \le M \end{aligned} \tag{24}$$

where $K' \cdot \mathbf{1}$ denotes a $1 \times J$ vector with all elements equal to K', $\mathbf{r} = [r_1\ r_2\ \dots\ r_J]$, and the set $\mathbf{U_x} = \{\mathbf{r} | K' \ge r_1 \ge x_1, K' \ge r_2 \ge x_2, \dots, K' \ge r_J \ge x_J\}$. Let $\widetilde{p}_i$ represents the failed transmission probability at the ith stage, which can be calculated as

$$\widetilde{p}_i = \begin{cases} 1 - \widetilde{\alpha}_{0,\mathbf{0}}, & i = 0, \\ \dfrac{1 - \widetilde{\alpha}_{i,\mathbf{0}}}{1 - \widetilde{\alpha}_{i-1,\mathbf{0}}}, & 0 < i \le M, \end{cases} \tag{25}$$

where $\mathbf{0}$ represents a $1 \times J$ vector with all elements equal to 0. By replacing p_i in (3) with $\widetilde{p}_i$ in (25), the parameters P_c and τ can be iteratively solved based on (3), (4), and (5). Moreover, $\widetilde{q}_{k,l}(z)$, $\widetilde{\alpha}_{i,\mathbf{x}}$, and $\widetilde{p}_i$ can also be obtained after acquiring the parameter P_c.

Furthermore, let $\widetilde{S}_i(z)$ be defined as the PGF of A-Encoded_MPDU's service time distribution on the condition that all the Encoded_MPDUs are successfully received at the ith backoff stage, and let $\widetilde{F}_{i,\mathbf{x}}(z)$ represent the PGF of total required time distribution on the condition that there are x_j failed RS blocks except for the first one in the jth Encode_MPDU for $1 \le j \le J$ at the ith backoff stage. Without the consideration of backoff delay, these two distributions can be, respectively, formulated as

$$\begin{aligned} \widetilde{S}_0(z) =& \frac{1 - P_c}{\widetilde{\alpha}_{0,0}} \left(\widetilde{q}_{K',0}(z) \cdot z^{L \cdot T_H} \right)^J \cdot z^{T_A}, \\ \widetilde{S}_i(z) =& \frac{1 - P_c}{\widetilde{\alpha}_{i,\mathbf{0}} - \widetilde{\alpha}_{i-1,\mathbf{0}}} \Bigg[\sum_{\substack{\mathbf{x} \in \mathbf{U_0} \\ (\mathbf{x} \ne \mathbf{0})}} \widetilde{\alpha}_{i-1,\mathbf{x}} \cdot \widetilde{F}_{i-1,\mathbf{x}}(z) \cdot \\ & \left(\prod_{j=1}^{J} \widetilde{q}_{x_j,0}(z) \cdot z^{L \cdot T_H} \right) \Bigg] \cdot z^{T_A},\ \ 0 < i \le M, \end{aligned} \tag{26}$$

and

$$\begin{aligned} \widetilde{F}_{0,\mathbf{x}}(z) =& \frac{1 - P_c}{\widetilde{\alpha}_{0,\mathbf{x}}} \left(\widetilde{q}_{K',K'}(z) \cdot z^{L \cdot T_H} \right)^J \cdot z^{T_A} + \frac{P_c}{\widetilde{\alpha}_{0,\mathbf{x}}} \cdot z^{T_{out}}, \\ & i = 0,\ \mathbf{x} = K' \cdot \mathbf{1} \\ \widetilde{F}_{0,\mathbf{x}}(z) =& \frac{1 - P_c}{\widetilde{\alpha}_{0,\mathbf{x}}} \prod_{j=1}^{J} \left(\widetilde{q}_{K',x_j}(z) \cdot z^{L \cdot T_H} \right) \cdot z^{T_A}, \\ & i = 0,\ \mathbf{x} \ne K' \cdot \mathbf{1} \\ \widetilde{F}_{i,\mathbf{x}}(z) =& \frac{1 - P_c}{\widetilde{\alpha}_{i,\mathbf{x}}} \Bigg[\sum_{\mathbf{r} \in \mathbf{U_x}} \widetilde{\alpha}_{i-1,\mathbf{r}} \cdot \widetilde{F}_{i-1,\mathbf{r}}(z) \\ & \prod_{j=1}^{J} \left(\widetilde{q}_{r_j,x_j}(z) \cdot z^{L \cdot T_H} \right) \Bigg] \cdot z^{T_A} \\ & + \frac{P_c}{\widetilde{\alpha}_{i,\mathbf{x}}} \cdot \widetilde{\alpha}_{i-1,\mathbf{x}} \cdot \widetilde{F}_{i-1,\mathbf{x}}(z) \cdot z^{T_{out}},\ i \ne 0, \end{aligned} \tag{27}$$

where T_H indicates the required time for sending one delimiter and the first RS block in an Encoded_MPDU. Note that the approximated formulations in (26) and (27) is obtained based on the condition that all the delimiters and the first RS blocks in the Encoded_MPDUs will be transmitted until the entire service finishes.

Furthermore, the three exclusive events that occur in a slot time with the existence of a specific WS in the backoff process will be the same as presented in (12). The corresponding time costs will also be identical to those in (15) except for the PGF $X(z)$ that represents event (b). Let

TABLE 1
System Parameters

Parameter	Value ASR-ARQ	Value AH-ARQ
Minimum window size (W)	32	
Maximum backoff stage (M)	5	
Retry limit	5	
Basic rate	15 Mbps	
Slot time (σ)	20 μs	
T_{SIFS}	10 μs	
T_{DIFS}	50 μs	
PHY header	24 Bytes	
Propagation delay (δ)	1 μs	
MPDU payload size	848 Bytes	
Delimiter	4 Bytes	
MAC header	28 Bytes	
RTS	20 Bytes	
CTS	14 Bytes	
BA	32 Bytes	56 Bytes

$\widetilde{X}(z)$ be defined as the PGF of required time distribution given the occurrence of event (b) for the proposed AH-ARQ algorithm, which can be acquired as

$$\widetilde{X}(z) = \sum_{i=0}^{M}\left\{\frac{b_{i,0}}{\tau}\left[\sum_{\substack{\mathbf{x}\in\mathbf{U_0}\\(\mathbf{x}\neq\mathbf{0})}}\left(\widetilde{P}_{X,i,\mathbf{x}}\cdot\prod_{j=1}^{J}\sum_{r=0}^{x_j}\widetilde{q}_{x_j,r}(z)\cdot z^{L\cdot T_H}\right)\cdot z^{T_A}\right]\right\}, \tag{28}$$

where

$$\widetilde{P}_{X,i,\mathbf{x}} = \begin{cases} 1, & i=0,\ \mathbf{x}=K'\cdot\mathbf{1},\\ 0, & i=0,\ \mathbf{x}\neq K'\cdot\mathbf{1},\\ \dfrac{\widetilde{\alpha}_{i-1,\mathbf{x}}}{1-\widetilde{\alpha}_{i-1,\mathbf{0}}}, & 0<i\leq M. \end{cases} \tag{29}$$

Moreover, the approximated PGF of slot time delay distribution $\widetilde{H}_d(z)$ for the AH-ARQ scheme can also be obtained by replacing $X(z)$ in (14) with $\widetilde{X}(z)$. The total backoff delay $\widetilde{H}_i(z)$ at the ith backoff stage for the AH-ARQ scheme will be of the same form as in (17). Let $\widetilde{\phi}_{succ,i}$ indicates the probability that all the Encoded_MPDUs have been successfully rec-eived at the ith backoff stage, which can be computed as

$$\widetilde{\phi}_{succ,i} = \begin{cases} \widetilde{\alpha}_{0,\mathbf{0}}, & i=0,\\ \widetilde{\alpha}_{i,\mathbf{0}}-\alpha_{i-1,\mathbf{0}}, & 0<i\leq M. \end{cases} \tag{30}$$

Finally, the PGF of total service time distribution, i.e., $\widetilde{T}(z)$, for the proposed AH-ARQ algorithm can be obtained as

$$\widetilde{T}(z) = \left(\sum_{i=0}^{M}\widetilde{\phi}_{succ,i}\cdot\widetilde{S}_i(z)\cdot\prod_{r=0}^{i}H_r(z)\right) + \left(\sum_{\substack{\mathbf{x}\in\mathbf{U_0}\\(\mathbf{x}\neq\mathbf{0})}}\widetilde{\alpha}_{M,\mathbf{x}}\cdot\widetilde{F}_{M,\mathbf{x}}(z)\right)\cdot\prod_{r=0}^{M}H_r(z). \tag{31}$$

4 Performance Evaluation

In this section, the performance of proposed ASR-ARQ and AH-ARQ schemes will be validated and compared via

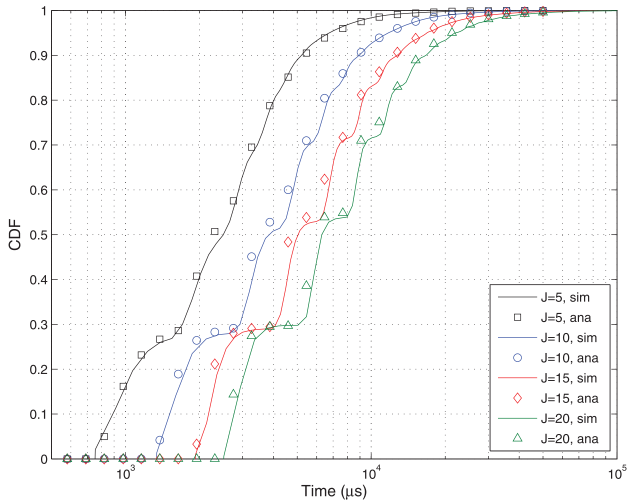

Fig. 7. Performance validation for ASR-ARQ scheme: CDF of service time distribution, i.e., inverse z-transform of $T(z)$, under SNR $= 10$ dB, MCS(16QAM, 1/2), and $L = 2$.

simulations. Additive white Gaussian noise is assumed for performance comparison under error-prone channels. Modulation and coding schemes (MCSs) are employed for the purpose of adapting channel quality which is evaluated by the received signal-to-noise ratio (SNR). Moreover, the effective BERs for MCSs can be precomputed by MATLAB tools in order to accelerate the simulation runs. Note that the notation "MCS(mod, R)" represents the modulation type mod and convolutional code with coding rate R that are applied for MCS. Note also that the reference data rate with MCS(16QAM, 1/2) is set to 60 Mbps, and the data rates with other MCSs can therefore be computed. A system C/C++ network simulation model is constructed by considering the AP based single-hop communications. As shown in Table 1, the MAC-defined parameters that are described in the IEEE 802.11n standard is adopted in both the analytical models and the simulations.

As illustrated from Figs. 7, 8, 9, 10, 11, and 12, the proposed analytical models for both the ASR-ARQ and AH-ARQ schemes are validated with simulation results. Note that three WSs, i.e., $N = 3$, are concurrently accessing the channel to communicate with the AP within the network. Fig. 7 shows the model validation for ASR-ARQ scheme via the CDF of service time by performing inverse z-transform of $T(z)$ in (19) under SNR $= 10$ dB, MCS(16QAM, 1/2), and the number of opportunities for A-MPDU transmissions $L = 2$. Each MPDU consists of 848-bytes information payload. Four different numbers of aggregated MPDUs within an A-MPDU are considered for model validation, i.e., $J = 5$, 10, 15, and 20. The results obtained from the analytical model are denoted as "ana"; while that from the simulations are represented as "sim." Intuitively, it is shown in the figure that the service time is increased as the number of aggregated MPDUs J is augmented. Fig. 8 illustrates the performance validation for the ASR-ARQ scheme for the number of aggregated MPDU $J = 5$, MCS(QPSK, 3/4), and $L = 2$ under different SNR values. It can be observed that the CDF of service time is decreased as the SNR value is increased. Fig. 9 displays

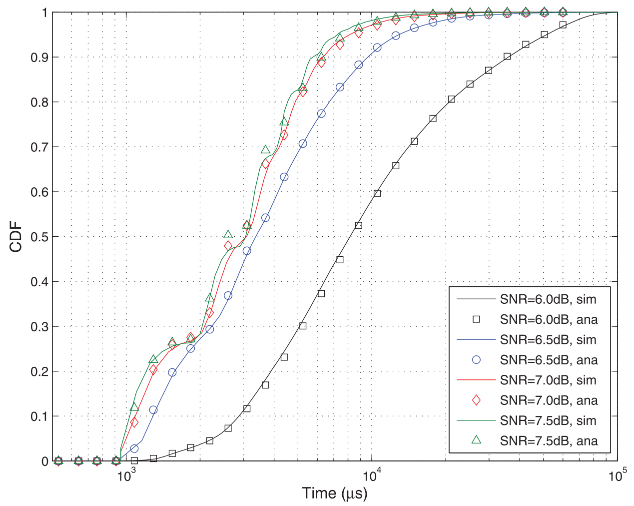

Fig. 8. Performance validation for ASR-ARQ scheme: CDF of service time distribution, i.e., inverse z-transform of $T(z)$, under $J = 5$, MCS(QPSK, 3/4), and $L = 2$.

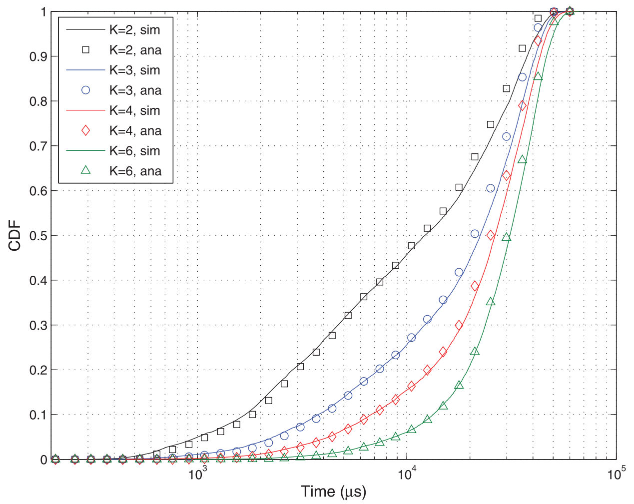

Fig. 10. Performance validation for AH-ARQ scheme: CDF of service time distribution, i.e., inverse z-transform of $\widetilde{T}(z)$, under SNR $= 4.5$ dB, MCS(QPSK, uncoded), and $L = 2$.

the performance validation condition on the number of aggregated MPDU $J = 5$, SNR $= 8.8$ dB and MCS(16QAM, 1/2) under different numbers of opportunities for A-MPDU transmissions L. It can be observed that there exists crossing effect between the curves, which denotes that larger value of L does not necessarily result in shorter service time. The reason is that both WS in concern and the other WSs possess the same opportunities to transmit their MPDUs, which may not result in shorter packet service time with larger value of L. For those WSs with shorter service time can benefit from larger L, which becomes a drawback for those WSs with longer service time. Moreover, as shown in all three figures, the results from the simulations and the analytical model are consistent with each other under different conditions.

On the other hand, considering that two Encoded_MPDUs are aggregated in an A-Encoded_MPDU, Fig. 10 illustrates the CDF of service time by conducting the inverse z-transform of $\widetilde{T}(z)$ in (31) for the proposed AH-ARQ algorithm with SNR $= 4.5$ dB, MCS(QPSK, uncoded), and $L = 2$ under different values of K; while Fig. 11 displays the performance validation for the scenario of $K = 4$, MCS(16QAM, 1/2), and $L = 2$ under different SNR values. Moreover, the performance validation under different L values are considered in Fig. 12 with $K = 4$, SNR $= 4.4$ dB, and MCS(QPSK, uncoded). Note that $K = 4$ corresponds to $K' = 3$. The RS$(255, 223)$ code over $GF(2^8)$ is constructed for the proposed AH-ARQ scheme via the primitive polynomial $1 + x^2 + x^3 + x^4 + x^8$. Each 848-bytes information payload contained in an original MPDU is partitioned into four RS blocks. The first RS block contains 191-bytes information octets and 28-bytes MAC header, and each of the remaining three RS block consists of 219-bytes information octets. Note that the remaining 4 bytes are occupied by the FCS for validation purpose. Similar to Figs. 7 and 8, longer service time will be incurred with

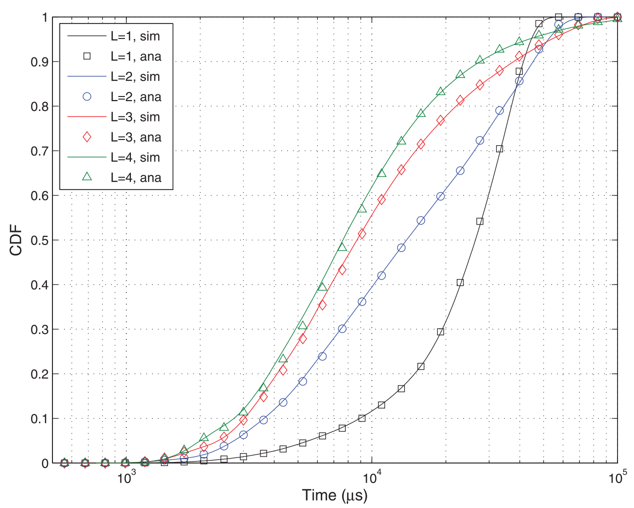

Fig. 9. Performance validation for ASR-ARQ scheme: CDF of service time distribution, i.e., inverse z-transform of $T(z)$, under $J = 5$, SNR $= 8.8$ dB, and MCS(16QAM, 1/2).

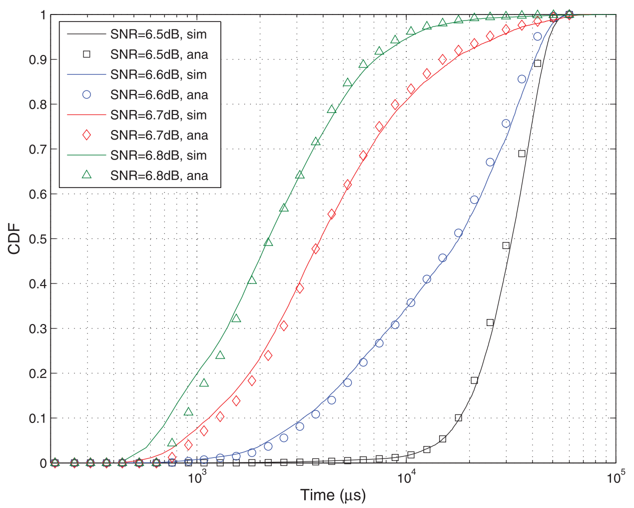

Fig. 11. Performance validation for AH-ARQ scheme: CDF of service time distribution, i.e., inverse z-transform of $\widetilde{T}(z)$, under the number of RS blocks $K = 4$, MCS(16QAM, 1/2) and $L = 2$.

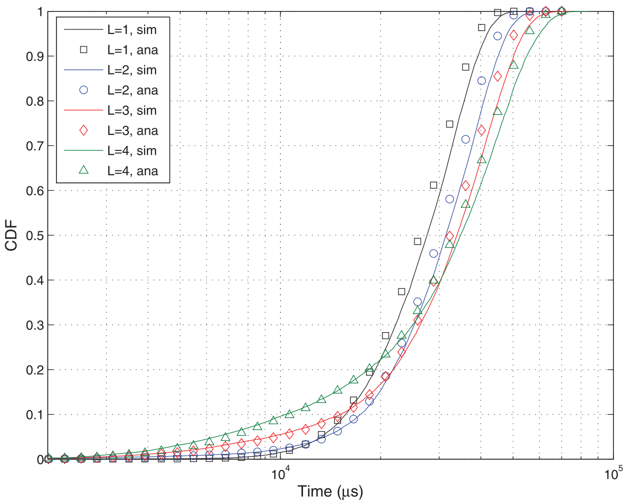

Fig. 12. Performance validation for AH-ARQ scheme: CDF of service time distribution, i.e., inverse z-transform of $\widehat{T}(z)$, under the number of RS block $K = 4$, SNR $= 4.4$ dB, and MCS(QPSK, uncoded).

either larger K or lower SNR value in Figs. 10 and 11, respectively. In Fig. 12, the crossing effect between different L curves is observed, which can also be explained similar to Fig. 9 for the ASR-ARQ scheme. It can be seen from all three figures that in most cases the proposed analytical model can match with the simulation results under different K, SNR, and L values.

Figs. 13, 14, 15, 16, 17, and 18 illustrate performance comparisons for proposed schemes under different parameter settings. If not further specified, the following parameters are set as the default values for performance comparison: number of WSs $N = 10$, number of transmission opportunities for A-MPDU/A-Encoded_MPDU $L = 2$, MCS(16QAM,1/2), aggregated MPDUs $J = 10$, number of RS blocks $K = 4$, and $\mathrm{RS}(255, 223)$ code. Fig. 13 shows the performance comparison for both the system throughput and mean service time under different SNR values with the number of aggregated MPDUs $J = 10$ and 20. The SW-ARQ scheme is also implemented in the simulations for

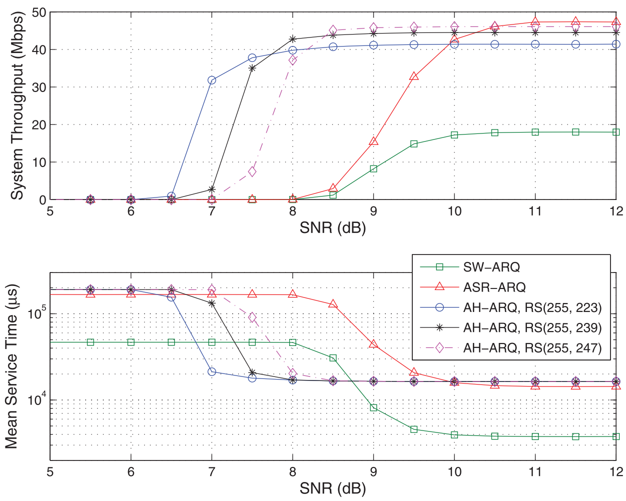

Fig. 14. Performance comparison: system throughput and mean service time versus SNR values under different RS code rates.

comparison purpose. The SW-ARQ approach denotes that only a single MPDU is delivered for data transmission, which can be regarded as a special case of the ASR-SRQ scheme by setting $J = 1$. It can be observed that the proposed AH-ARQ algorithm outperforms the other two schemes under lower SNR values, i.e., for SNR < 10 dB. The reason is that there is higher probability for the AH-ARQ scheme to correct packet errors compared to the other mechanisms without RS codes since packet transmission tends to fail under lower SNR environments. Moreover, the system throughput of the AH-ARQ approach can maintain at the same level under different SNR values; while the performances of the other two schemes significantly drop with decreased SNR values. On the other hand, the proposed AH-ARQ algorithm is inferior to the ASR-ARQ scheme under higher SNR values, i.e., SNR > 10 dB. The redundant FEC field in the proposed AH-ARQ scheme will become communication overheads under better channel conditions. It can also be observed that both the proposed aggregation-based algorithms, i.e., the AH-ARQ

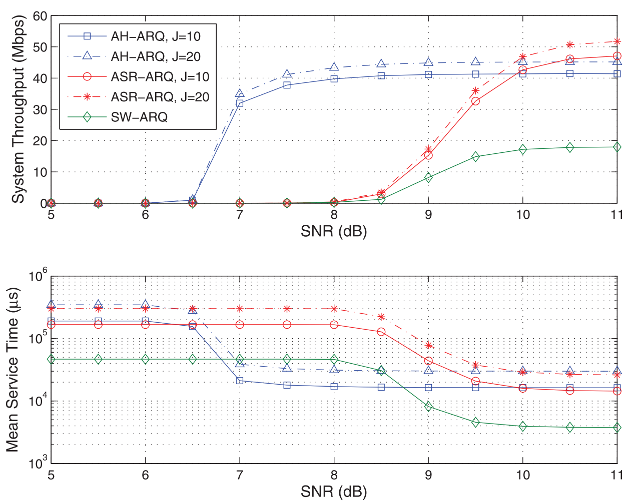

Fig. 13. Performance comparison: system throughput and mean service time versus SNR values under different numbers of MPDUs (J).

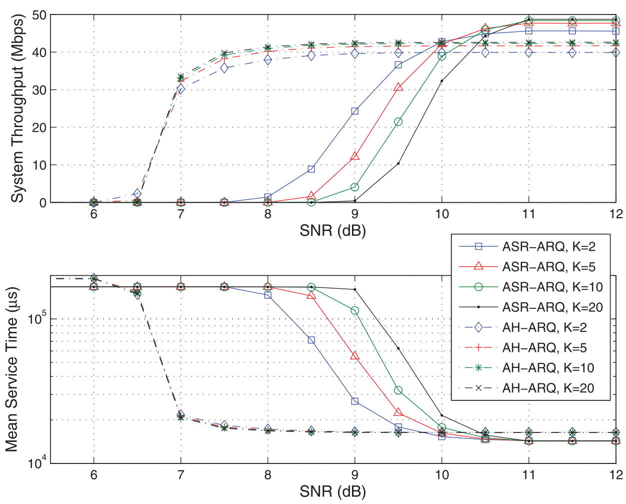

Fig. 15. Performance comparison: system throughput and mean service time versus SNR values under different MPDU/Encoded_MPDU sizes with a roughly fixed A-MPDU/A-Encoded_MPDU length.

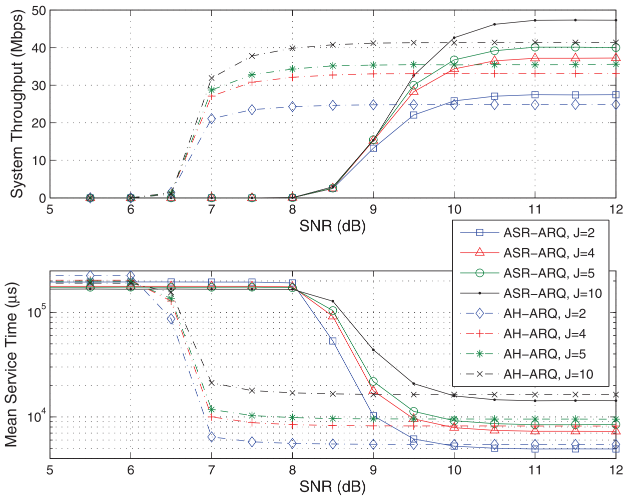

Fig. 16. Performance comparison: system throughput and mean service time versus SNR values under different numbers of MPDUs (J) with a roughly fixed TXOP duration.

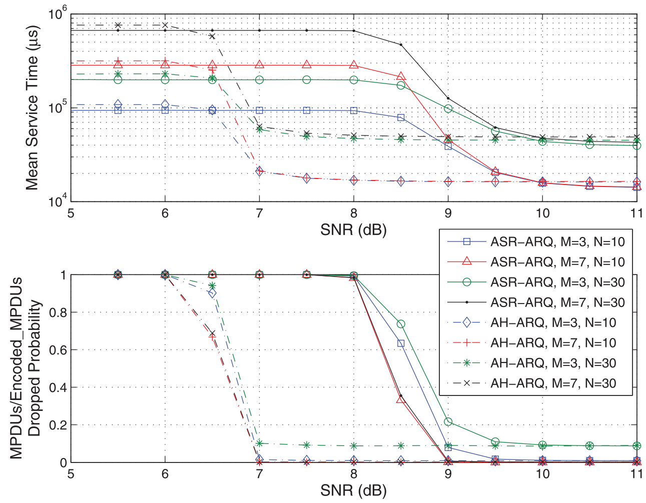

Fig. 18. Performance comparison: mean service time and MPDUs/Encoded_MPDUs dropped probability versus SNR values under different retry limits (M) and number of WSs (N).

and ASR-ARQ schemes, can provide better performance compared to the SW-ARQ scheme since MPDU aggregation can effectively improve channel utilization. Moreover, under the same scheme, system throughput can be enhanced with larger number of aggregated MPDUs J due to the increased channel utilization. However, elongated mean service time is required under larger J since each WS will spend more time both on its own data transmission and waiting for other WS's data delivery.

Fig. 14 displays the performance comparison for both the system throughput and mean service time with different RS coding rates. For fair comparison, the sizes of both MPDU and Encoded_MPDU are fixed as 1,020 bytes. Therefore, the payloads for ASR-ARQ/SW-ARQ mechanisms are $1020 - 28 = 992$ bytes; while the payloads for AH-ARQ scheme with RS(255,223), RS(255,239), and RS(255,247) will be 848, 912, 944 bytes, respectively. Note that the 848-bytes MPDU is computed from 219 (payload per RS block) $\times$ $(K = 4) - 28$ (MAC header) $= 848$, where the number of RS blocks is chosen as $K = 4$. It can be seen from both figures that the AH-ARQ scheme with lower RS coding rate outperforms the other algorithms under lower SNR channel since the scheme with lower RS coding rate can protect more information bytes. For instance, the throughput of AH-ARQ scheme with RS(255,223) can still be maintained at around 32 Mbps even if the SNR value approaches 7 dB; while that from the other schemes drops quickly under low SNR values. On the other hand, the ASR-ARQ scheme will provide higher system throughput under high SNR values due to the required FEC overhead from the AH-ARQ approach. Moreover, under higher SNR channel, the AH-ARQ scheme with higher RS coding rate will provide larger system throughput than that with lower RS coding rate since low RS coding rate will incur reduced number of successfully received information bytes.

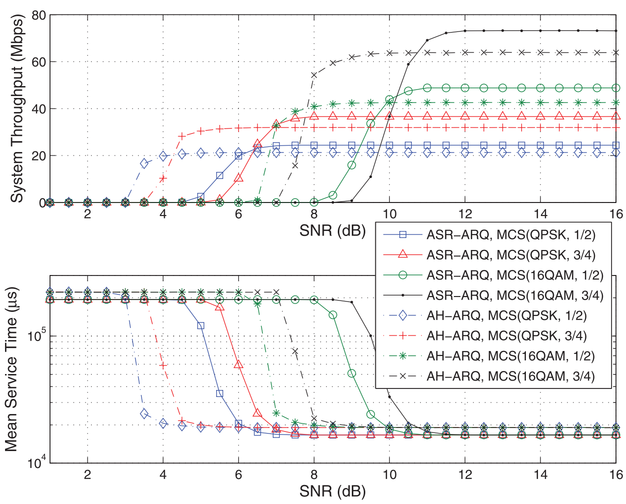

Fig. 17. Performance comparison: system throughput and mean service time versus SNR values under different MCSs.

As shown in Figs. 13 and 14, the performance of SW-ARQ scheme is inferior to the proposed ASR-ARQ and AH-ARQ schemes under most cases. Therefore, the SW-ARQ scheme will be omitted in the following plots to provide better performance comparisons between the ASR-ARQ and AH-ARQ algorithms. Fig. 15 displays the performance comparison for both the system throughput and mean service time under different MPDU/Encoded_MPDU sizes with a roughly fixed A-MPDU/A-Encoded_MPDU length. For fair comparison, both the MPDU and Encoded_MPDU payload sizes for curve K are computed as $219 \times K - 28$ that follows the computation for the RS block, even though it is not adopted in MDPU for the ASR-ARQ scheme. In order to approximately fix the length of A-MPDU/A-Encoded_MPDU, the number of aggregated MPDUs/Encoded_MPDUs J in an A-MPDU/A-Encoded_MPDU is calculated by $40/K$. It can be observed that larger MPDU size can lead to higher system throughput for the ASR-ARQ scheme under higher SNR values, which is mainly caused by higher channel utilization. However, larger payload size results in worse performance under lower SNR values due to higher failure rate for transmitting larger MPDUs. On the other hand, the AH-ARQ scheme with larger Encoded_MPDU size outperforms that with smaller payload size under different SNR values due to the reason that each Encoded_MPDU is divided into several self-correcting RS blocks. On the other hand, the number of aggregated MPDUs/Encoded_MPDUs J can provide complementary effect as the MPDU/Encoded_MPDU size to the system performance. For the AH-ARQ scheme, adding J value will cause augmentation of the MAC header overhead which slightly decreases the throughput performance for the case $K = 2$ compared to the curve $K = 20$. Moreover, for ASR-ARQ scheme, larger J value (e.g., $K = 2$ case) can conquer the worse channel condition with its MAC header protection, which lead to higher system throughput. In addition, it can still be observed from both system throughput and mean service time that the proposed AH-ARQ algorithm can outperform the ASR-ARQ scheme under worse channel condition; while the ASR-ARQ protocol is slightly superior to the AH-ARQ scheme under better channel condition.

Fig. 16 shows the performance comparison for both the system throughput and mean service time considering the tradeoff between the number of MPDUs in an A-MPDU (i.e., J) and the number of A-MPDUs (L) in a fixed TXOP duration. The maximum transmission opportunities L for A-MPDU/A-Encoded_MPDU transmissions can be computed as $20/J$ such that the TXOP duration can be approximately fixed. In other words, smaller transmission opportunities L will be acquired if the number of MPDU/Encoded_MPDU J is enlarged. It can be seen from the figure that larger J value leads to higher system throughput for both the ASR-ARQ and AH-ARQ schemes since large J value can effectively enhance channel utilization. Therefore, the throughput performance is almost dominated by the J value rather than L due to the reason that adding L may furthermore cause extra communication overheads, e.g., ACK frame and SIFS interval. Moreover, it is not required for the WS to completely utilize all L opportunities if its packets have all been successfully transmitted. Hence, it can be seen that the throughput performance can be effectively enhanced by increasing J compared to the augmentation of L.

Fig. 17 shows the performance comparison for both the system throughput and mean service time for different MCSs. Note that the data rates of MCS(QPSK, 1/2), MCS(QPSK, 3/4), MCS(16QAM, 1/2), and MCS(16QAM, 3/4) are respectively 30 Mbps, 45 Mbps, 60 Mbps, and 90 Mbps. For fair comparison, the corresponding number of aggregated MPDUs J are, respectively, chosen as 6, 9, 12, and 18 in order to result in an identical TXOP period. It can be observed from the perspectives of both system throughput and mean service time that MCS with lower data rate can provide better performance than that with higher data rate under lower SNR values. The reason is that adopting MCS with lower data rate can decrease BER compared to that with higher data rate under the same SNR value. On the other hand, adopting MCS with higher date rate can lead to better performance compared to that with lower data rate under higher SNR values since more MPDUs can be accommodated within a single TXOP duration. From Fig. 17, it can be seen that the proposed AH-ARQ scheme provides better performance compared to the ASR-ARQ method under worse channel conditions.

Finally, Fig. 18 shows the performance comparison for both mean service time and MPDUs/Encoded_MPDUs dropped probability under different retry limits M and numbers of WSs N. Note that system throughput is not considered in this figure since mean service time and MPDUs/Encoded_MPDUs dropped probability are observed to be more sensitive to the variations of parameters M and N. It can be seen from the upper plot that longer service time will be acquired in both algorithms under larger M and N values, i.e., the case with $M = 7$ and $N = 30$. On the other hand, it is intuitive that lower MPDUs/Encoded_MPDUs dropped probability can be achieved with larger value of retry limit M, i.e., the cases with $M = 7$ in the lower plot. Furthermore, it can still be observed that the proposed AH-ARQ scheme is superior to the ASR-ARQ protocol under different SNR, M, and N values.

5 Conclusion

In this paper, two automatic repeat request mechanisms are proposed with the consideration of frame aggregation under the IEEE 802.11n networks. The aggregated selective repeat ARQ protocol is proposed by incorporating the conventional stop-and-wait ARQ scheme; while the aggregated hybrid ARQ algorithm further enhances throughput performance by adopting the Reed-Solomon block code for error correction under worse channel quality. Analytical models are constructed to evaluate the performance of proposed ASR-ARQ and AH-ARQ algorithms with the consideration of interfering stations. Simulations are also conducted to validate and compare the effectiveness of proposed ARQ mechanisms via both the mean service time and throughput performance. Numerical results show that the proposed AH-ARQ protocol can outperform the other schemes under worse channel condition; while the proposed ASR-ARQ protocol is superior to the other mechanisms under better channel condition.

Acknowledgments

This work was in part funded by the Aiming for the Top University and Elite Research Center Development Plan, NSC 99-2628-E-009-005, the MediaTek research center at National Chiao Tung University, and the Telecommunication Laboratories at Chunghwa Telecom Co. Ltd, Taiwan.

References

[1] *IEEE 802.11 WG, IEEE Std 802.11a-1999 (R2003): Part 11: Wireless LAN Medium Access Control (MAC) and Physical Layer (PHY) Specifications: High-Speed Physical Layer in the 5 GHz Band*, IEEE, 2003.

[2] *IEEE 802.11 WG, IEEE Std 802.11b-1999 (R2003): Part 11: Wireless LAN Medium Access Control (MAC) and Physical Layer (PHY) Specifications: Higher-Speed Physical Layer Extension in the 2.4 GHz Band*, IEEE, 2003.

[3] *IEEE 802.11 WG, IEEE Std 802.11g-2003: Part 11: Wireless LAN Medium Access Control (MAC) and Physical Layer (PHY) Specifications: Amendment 4: Further Higher Data Rate Extension in the 2.4 GHz Band*, IEEE, 2003.

[4] *IEEE 802.11 WG, IEEE Std 802.11e-2005: Part 11: Wireless LAN Medium Access Control (MAC) and Physical Layer (PHY) Specifications: Amendment 8: Medium Access Control (MAC) Quality of Service Enhancements*, IEEE, 2005.

[5] *IEEE 802.11 WG, IEEE P802.11n-2009: Part 11: Wireless LAN Medium Access Control (MAC) and Physical Layer (PHY) Specifications: Amendment 5: Enhancements for Higher Throughput*, IEEE, Oct. 2009.

[6] S. Abraham, A. Meylan, and S. Nanda, "802.11n MAC Design and System Performance," *Proc. IEEE Int'l Conf. Comm. (ICC)*, vol. 5, May 2005.

[7] Y. Li, S.W. Kim, J.K. Chung, and H.G. Ryu, "SFBC-Based MIMO OFDM and MIMO CI-OFDM Systems in the Nonlinear and NBI Channel," *Proc. IEEE Int'l Conf. Comm., Circuits and Systems (ICCCAS)*, vol. 2, pp. 898-901, June 2006.

[8] Y. Li, X. Wang, and S.A. Mujtaba, "Impact of Physical Layer Parameters on the MAC Throughput of IEEE 802.11 Wireless LANs," *Proc. Record of the 38th Asilomar Conf. Signals, Systems and Computers Conf. (ACSSC)*, vol. 2, pp. 1468-1472, Nov. 2004.

[9] D. Skordoulis, Q. Ni, H.H. Chen, A.P. Stephens, C. Liu, and A. Jamalipour, "IEEE 802.11n MAC Frame Aggregation Mechanisms for Next-Generation High-Throughput WLANs," *IEEE Wireless Comm.*, vol. 15, no. 1, pp. 40-47, Feb. 2008.

[10] B. Ginzburg and A. Kesselman, "Performance Analysis of A-MPDU and A-MSDU Aggregation in IEEE 802.11n," *Proc. IEEE Sarnoff Symp.*, May 2007.

[11] S. Parthasarathy and Q. Zeng, "A Novel Adaptive Scheme to Improve the Performance of the IEEE 802.11n WLANs," *Proc. IEEE 21st Int'l Conf. Advanced Information Networking and Applications Workshops (AINAW)*, vol. 2, May 2007.

[12] S. Kim, S. Choi, Y. Kim, and K. Jang, "MCCA: A High-Throughput MAC Strategy for Next-Generation WLANs," *IEEE Wireless Comm.*, vol. 15, no. 1, pp. 32-39, Feb. 2008.

[13] D.L. Lu and J.F. Chang, "Analysis of ARQ Protocols via Signal Flow Graphs," *IEEE Trans. Comm.*, vol. 37, no. 3, pp. 245-251, Mar. 1989.

[14] Y. Hua and Z. Niu, "An Analytical Model for IEEE 802.11 WLANs with NAK-Based ARQ Mechanism," *Proc. Asia-Pacific Conf. Comm. (APCC)*, pp. 277-280, Oct. 2007.

[15] J.B. Seo, N.H. Park, H.W. Lee, and C.H. Cho, "Impact of an ARQ Scheme in the MAC/LLC Layer on Upper-Layer Packet Transmissions over a Markovian Channel," *Proc. IEEE 63rd Vehicular Technology Conf. (VTC-Spring)*, vol. 4, May 2006.

[16] K.C. Beh, A. Doufexi, and S. Armour, "Performance Evaluation of Hybrid ARQ Schemes of 3GPP LTE OFDMA System," *Proc. IEEE 18th Int'l Symp. Indoor and Mobile Radio Comm. (PIMRC)*, pp. 1-5, Sept. 2007.

[17] E. Malkamaki, D. Mathew, and S. Hamalainen, "Performance of Hybrid ARQ Techniques for WCDMA High Data Rates," *Proc. IEEE 53rd Vehicular Technology Conf. (VTC-Spring)*, vol. 4, pp. 2720-2724, May 2001.

[18] T.F. Wong, L. Gao, and T.M. Lok, "A Type-I Hybrid ARQ Protocol over Optimal-Sequence CDMA Link," *Proc. IEEE 21st Century Military Comm. Conf. (MILCOM)*, vol. 1, pp. 559-563, Oct. 2001.

[19] J.F. Cheng, Y.P.E. Wang, and S. Parkvall, "Adaptive Incremental Redundancy [WCDMA Systems]," *Proc. IEEE 58th Vehicular Technology Conf. (VTC-Fall)*, vol. 2, Oct. 2003.

[20] Q. Chen and P. Fan, "On The Performance of Type-III Hybrid ARQ with RCPC Codes," *Proc. IEEE 14th Int'l Symp. Indoor and Mobile Radio Comm. (PIMRC)*, vol. 2, pp. 1297-1301, Sept. 2003.

[21] R. Guo and J.L. Liu, "BER Performance Analysis of RCPC Encoded MIMO-OFDM in Nakagami-m Channels," *Proc. IEEE Int'l Conf. Information Acquisition (ICIA)*, pp. 1416-1420, Aug. 2006.

[22] D.N. Rowitch and L.B. Milstein, "On the Performance of Hybrid FEC/ARQ Systems Using RCPT Codes," *IEEE Trans. Comm.*, vol. 48, no. 6, pp. 269-281, June 2000.

[23] J.G. Proakis, *Digital Communication*, fourth ed. McGraw-Hill, 2001.

[24] U. Cheng, "On the Continued Fraction and Berlekamp's Algorithm," *IEEE Trans. Information Theory*, vol. 30, no. 3, pp. 541-544, May 1984.

[25] M.A. Khan, S. Afzal, and R. Manzoor, "Hardware Implementation of Shortened (48,38) Reed Solomon Forward Error Correcting Code," *Proc. Seventh Int'l Multi Topic Conf. (INMIC 03)*, pp. 90-95, Dec. 2003.

[26] G. Bianchi, "Performance Analysis of the IEEE 802.11 Distributed Coordination Function," *IEEE J. Selected Areas in Comm.*, vol. 18, no. 3, pp. 535-547, Mar. 2000.

[27] O. Tickoo and B. Sikdar, "Queueing Analysis and Delay Mitigation in IEEE 802.11 Random Access MAC Based Wireless Networks," *Proc. IEEE INFOCOM*, vol. 2, pp. 1404-1413, Mar. 2004.

[28] Y. Zheng, K. Lu, D. Wu, and Y. Fang, "Performance Analysis of IEEE 802.11 DCF in Binary Symmetric Channels," *Proc. IEEE GLOBECOM*, vol. 5, pp. 3144-3148, Nov. 2005.

[29] Q. Ni, T. Li, T. Turletti, and Y. Xiao, "Saturation Throughput Analysis of Error-Prone 802.11 Wireless Networks," *J. Wireless Comm. and Mobile Computing*, vol. 5, no. 8, pp. 945-956, Dec. 2005.

[30] Y. Lin and V.W.S. Wong, "Frame Aggregation and Optimal Frame Size Adaptation for IEEE 802.11n WLANs," *Proc. IEEE GLOBECOM*, vol. 5, pp. 1-6, Nov. 2006.

[31] S. Kuppa and G.R. Dattatreya, "Modeling and Analysis of Frame Aggregation in Unsaturated WLANs with Finite Buffer Stations," *Proc. IEEE Int'l Conf. Comm. (ICC)*, pp. 967-972, June 2006.

[32] C.W. Liu and A.P. Stephens, "An Analytic Model for Infrastructure WLAN Capacity with Bidirectional Frame Aggregation," *Proc. IEEE Wireless Comm. and Networking Conf. (WCNC)*, vol. 1, pp. 113-119, Mar. 2005.

[33] T. Li, Q. Ni, and Y. Xiao, "Investigation of the Block ACK Scheme in Wireless Ad-Hoc Networks," *J. Wireless Comm. and Mobile Computing*, vol. 6, no. 6, pp. 877-888, Sept. 2006.

[34] T. Li, Q. Ni, D. Malone, D. Leith, Y. Xiao, and T. Turletti, "Aggregation with Fragmentation Retransmission for Very High-Speed Wireless LANs," *IEEE/ACM Trans. Networking*, vol. 17, no. 2, pp. 591-604, Apr. 2009.

[35] S. Choi and K.G. Shin, "A Class of Adaptive Hybrid ARQ Scheme for Wireless Links," *IEEE Trans. Vehicular Technology*, vol. 50, no. 3, pp. 777-790, May 2001.

[36] S. Choi, Y. Choi, and I. Lee, "IEEE 802.11 MAC-Level FEC with Retransmission Combining," *IEEE Trans. Wireless Comm.*, vol. 5, no. 1, pp. 203-211, Jan. 2006.

[37] Y. Choi and S. Choi, "Above-MAC FEC Scheme in IEEE 802.11 WLAN," *Proc. IEEE Asia Pacific Wireless Comm. Symp. (APWCS)*, Aug. 2005.

[38] E. Berlekamp, *Algebraic Coding Theory*. McGraw-Hill, 1968.

[39] H.V. Zoran and S. Boris, "Saturation Throughput - Delay Analysis of IEEE 802.11 DCF in Fading Channel," *Proc. IEEE Int'l Conf. Comm. (ICC)*, vol. 1, pp. 121-126, May 2003.

[40] Z. Eustathia and A. Theodore, "CSMA/CA Performance under High Traffic Conditions: Throughput and Delay Analysis," *Computer Comm.*, vol. 25, no. 3, pp. 313-321, Feb. 2002.

[41] S. Ci, H. Sharif, and P. Mahasukhon, "Evaluating Saturation Throughput Performance of the IEEE 802.11 MAC under Fading Channels," *Proc. IEEE Second Int'l Conf. Broadband Networks (BROADNETS)*, vol. 1, pp. 676-681, Oct. 2005.

[42] J.S. Vardakas, M.K. Sidiropoulos, and M.D. Logothetis, "Performance Behaviour of IEEE 802.11 Distributed Coordination Function," *IET Circuits, Devices and Systems*, vol. 2, no. 1, pp. 50-59, 2008.

[43] H. Wu, Y. Peng, K. Long, S. Cheng, and J. Ma, "Performance of Reliable Transport Protocol over IEEE 802.11 Wireless LAN: Analysis and Enhancement," *Proc. IEEE INFOCOM*, vol. 2, pp. 599-607, Jun. 2002.

Jia-Shi Lin received the BS degree from National Tsing Hua University, Hsinchu, Taiwan, in 2007. Since 2007, he has been working toward the PhD degree in the Department of Electrical Engineering, National Chiao Tung University, Hsinchu, Taiwan. His current research interests include game theory, MAC protocol design, wireless local area networks, and cognitive radio networks. He is a student member of the IEEE.

Kai-Ten Feng received the BS degree from National Taiwan University, Taipei, in 1992, the MS degree from the University of Michigan, Ann Arbor, in 1996, and the PhD degree from the University of California, Berkeley, in 2000. Between 2000 and 2003, he was an in-vehicle development manager/senior technologist with OnStar Corporation, a subsidiary of General Motors Corporation, where he worked on the design of future telematics platforms and in-vehicle networks. Since August 2011, he has been a full professor with the Department of Electrical and Computer Engineering, National Chiao Tung University (NCTU), Hsinchu, Taiwan, where he was an associate professor and assistant professor from August 2007 to July 2011 and from February 2003 to July 2007, respectively. From July 2009 to March 2010, he was a visiting scholar with the Department of Electrical and Computer Engineering, University of California at Davis. He has also been the convener of the NCTU Leadership Development Program since August 2011. Since October 2011, he has been serving as the director of the Digital Content Production Center at the same university. His current research interests include broadband wireless networks, cooperative and cognitive networks, smart phone and embedded system designs, wireless location technologies, and intelligent transportation systems. He received the Best Paper Award from the Spring 2006 IEEE Vehicular Technology Conference, which ranked his paper first among the 615 accepted papers. He also received the Outstanding Youth Electrical Engineer Award in 2007 from the Chinese Institute of Electrical Engineering and the Distinguished Researcher Award from NCTU in 2008, 2010, and 2011. He has served on the technical program committees in various international conferences. He is a member of the IEEE and the IEEE Computer Society.

Yu-Zhi Huang received the BS degree in electrical engineering from National Tsing Hua University, Taiwan, in 2006, and the MS degree in the Department of Communication Engineering at National Chiao Tung University, Taiwan, in 2008. Currently, he is working for Holtek Semiconductor Inc. in Taipei, Taiwan. His research interests include MAC protocol design in WLAN systems, cross layer optimization, error control techniques, and the implementation of multicast routing protocols.

Li-Chun Wang received the BS degree from National Chiao Tung University, Taiwan, R.O.C. in 1986, the MS degree from National Taiwan University in 1988, and the MSc and PhD degrees from the Georgia Institute of Technology, Atlanta, in 1995, and 1996, respectively, all in electrical engineering. From 1990 to 1992, he was with the Telecommunications Laboratories of the Ministry of Transportations and Communications in Taiwan (currently the Telecom Labs of Chunghwa Telecom Co.). In 1995, he was affiliated with Bell Northern Research of Northern Telecom, Inc., Richardson, Texas. From 1996 to 2000, he was with AT&T Laboratories, where he was a senior technical staff member in the Wireless Communications Research Department. In August 2000, he joined the Department of Electrical and Computer Engineering of National Chiao Tung University in Taiwan and is the current chairman of that department. His current research interests include the areas of radio resource management and cross-layer optimization techniques for wireless systems, heterogeneous wireless network design, and cloud computing for mobile applications. He was a corecipient (with Gordon L. Stüber and Chin-Tau Lea) of the 1997 IEEE Jack Neubauer Best Paper Award for his paper "Architecture Design, Frequency Planning, and Performance Analysis for a Microcell/Macrocell Overlaying System," *IEEE Transactions on Vehicular Technology*, vol. 46, no. 4, pp. 836-848, 1997. He has published more than 150 journal and international conference papers. He served as an associate editor for the *IEEE Transactions on Wireless Communications* from 2001 to 2005, as a guest editor of the special issue on "mobile computing and networking" for the *IEEE Journal on Selected Areas in Communications* in 2005, and on "radio resource management and protocol engineering in future IEEE broadband networks" for *IEEE Wireless Communications Magazine* in 2006. He holds nine US patents. He was elected as an IEEE fellow in 2011 for his contributions to cellular architectures and radio resource management in wireless networks.